

## PRELIMINARY ANNUAL ESTIMATES OF REGIONAL NITRATE SUPPLY IN THE SOUTHERN BENGUELA USING COASTAL SEA LEVEL FLUCTUATIONS AS A PROXY FOR UPWELLING

H. N. WALDRON\*, T. A. PROBYN† and G. B. BRUNDRIT\*

First-order estimates of annual potential new production are presented for the southern Benguela upwelling region for the decade of the 1980s. Using satellite images of sea surface temperature and a 10-year record of sea level, preliminary estimates of potential new production for 12-month periods between May and June inclusive were made for the period 1980/81 to 1989/90. The annual period was selected so as to encompass the upwelling season (austral spring and summer) and to optimize the interaction between upwelling and biological response. The range of these estimates was  $5.16 \times 10^{13}$  to  $6.19 \times 10^{13}$  gC·year<sup>-1</sup>, with a mean of  $5.60 \times 10^{13}$  gC·year<sup>-1</sup>. The trend in the estimates was found to be consistent with related variables and their validity, in terms of order of magnitude, was tested against <sup>15</sup>N<sub>3</sub>-N uptake rates measured in the southern Benguela and scaled to a regional level. In addition, they were subjected to an intra- and inter-regional comparison.

The Benguela upwelling system off the west coast of southern Africa is one of four major eastern boundary currents (others are located off the Californian, Peruvian/Chilean and North-West African coasts). It is characterized by equatorward winds with concomitant upwelling of cold, nutrient-rich water adjacent to the coast, resulting in enhanced levels of production at all trophic levels (Andrews and Hutchings 1980, Nelson and Hutchings 1983, Shannon 1985, Chapman and Shannon 1985, Shannon and Pillar 1986, Crawford *et al.* 1987).

Dugdale and Goering (1967) apportioned total primary production between “new” and “regenerated” production, depending on the nitrogenous sources to, and its cycling within, the euphotic zone. Through the use of <sup>15</sup>N labelling techniques, it was shown that nitrogen available to the phytoplankton could be divided between newly incorporated nitrogen (NO<sub>3</sub>-N or N<sub>2</sub>) and metabolically recycled nitrogen (NH<sub>4</sub>-N or dissolved organic-N, mainly urea). Budgetary considerations dictate that new nitrogen (*viz* NO<sub>3</sub>-N) must enter the productive surface layer at a rate sufficient to equal or exceed the export of organic nitrogen in order to prevent the ecosystem running down. Upwelling system dynamics dictate that this precondition is met.

New production is the proportion of total primary production that relies on the uptake of NO<sub>3</sub>-N, whereas potential new production assumes that all the NO<sub>3</sub>-N available to primary producers is assimilated (Waldron and Probyn 1992). The regional estimate of annual potential new production was therefore obtained by quantifying, over a 12-month period, the supply of

NO<sub>3</sub>-N to the productive surface waters of the coastal zone in an area designated as the southern Benguela upwelling system.

The Benguela system is driven by the interaction between zonal shifts of the South Atlantic high pressure system, the seasonally oscillating pressure field over southern Africa and the belt of east-moving cyclones to the south. This results in a seasonal pattern of upwelling in the southern region of the Benguela, reaching its maximum during spring and summer (Shannon 1966, Andrews and Hutchings 1980). Upwelling is perennial in the central and northern regions, with a maximum in spring/summer and a minimum in late winter/spring (Shannon 1985). Taking those factors into account, together with physical considerations based on the geographical distribution of upwelling cells (Lutjeharms and Meeuwis 1987), and the biological boundary between northern and southern anchovy fish stocks (Cruickshank *et al.* 1990), the zonal range of the southern Benguela is defined here as lying between 29 and 35°S. Its meridional range is defined by the seaward extent of upwelling-derived water.

In order to arrive at annual estimates of NO<sub>3</sub>-N supply (*i.e.* potential new production) to the productive surface layer of the Benguela, it was first necessary to quantify the amount of NO<sub>3</sub>-N introduced over a range of upwelling events. This was achieved in a manner similar to that of Waldron and Probyn (1992) by making use of the regionally specific relationship between sea surface temperature (SST) and depth-integrated NO<sub>3</sub>-N (over the nominal euphotic zone), in combination with a series of satellite images of SST

\* Department of Oceanography, University of Cape Town, Private Bag, Rondebosch 7701, South Africa. E-mail: waldron@physci.uct.ac.za

† Formerly University of Cape Town; now Sea Fisheries Research Institute, Private Bag X2, Rogge Bay 8012, South Africa.

E-mail: tprobyn@sfrri.wcape.gov.za

taken during upwelling events. An extrapolation to the annual scale necessitated the identification of a proxy for upwelling, related to event-scale estimates of potential new production that could possibly be used as an upwelling index. In the present study, the fluctuation of tidal-filtered and pressure-adjusted coastal sea level was found to be a possible proxy. It was used to obtain the cumulative amount of  $\text{NO}_3\text{-N}$  in a series of 12-month periods, providing first-order annual estimates of potential new production for the 1980s. This paper presents the preliminary findings using this methodology. The robustness of the method was tested using published regional values and measured rates of  $\text{NO}_3\text{-N}$  uptake.

## MATERIAL AND METHODS

### Event-scale estimates of potential new production

A dataset of temperature ( $^{\circ}\text{C}$ ) v.  $\text{NO}_3\text{-N}$  ( $\text{mmol}\cdot\text{m}^{-3}$ ) sampled vertically at 423 stations in the southern Benguela was compiled from archived data from the South African Data Centre for Oceanography (SADCO) and the Sea Fisheries Research Institute (SFRI). Using these data, the primary objective was to establish a significant, negatively correlated relationship between SST and  $\text{NO}_3\text{-N}$ , integrated over the depth range of the nominal euphotic zone ( $\text{mmol}\text{NO}_3\text{-N}\cdot\text{m}^{-2}$ ). Measured euphotic zone depths were not available from all stations in the dataset. Therefore, reported values from Shannon (1985), Brown and Hutchings (1987) and Estrada and Marrasé (1987) were used to establish that 30 m was a realistic (and possibly conservative) southern Benguela euphotic zone depth (Waldron and Probyn 1992), or at least the depth to which  $\text{NO}_3\text{-N}$  would be available to primary producers. Where the sampling depth at a particular station was not 30 m, a linearly interpolated concentration of  $\text{NO}_3\text{-N}$  ( $\text{mmol}\cdot\text{m}^{-3}$ ) was obtained from adjacent values. Integrated values for each station were calculated and regressed against the appropriate SST value.

Surface water of upwelling origin was assumed to vary between 10 and 17 $^{\circ}\text{C}$ , which takes into account sun-warming of newly upwelled water over an upwelling cycle. Typically, water < 17 $^{\circ}\text{C}$  is found inshore of the upwelling front in the southern Benguela. One satellite image of SST taken during a prominent and relatively cloud-free upwelling event was selected for each year between 1984/1985 and 1993/1994. Financial constraints prevented the selection of more than one image for each year. To determine SST, advanced very high resolution radiometer (AVHRR) data from the TIROS/NOAA series of polar-orbiting

satellites were obtained from the South African Satellite Application Centre, Hartebeeshoek. Raw AVHRR data from the visible spectral band (0.58–0.68  $\mu\text{m}$ ) and SST calibrated data from bands four and five in the thermal infra-red (10.5–11.5 and 11.5–12.5  $\mu\text{m}$ ) were obtained for the 10 selected images. The data were processed using the PC-SEAPAK software package developed at the NASA Goddard Space Flight Centre (McClain *et al.* 1992). These were transformed to an equirectangular projection with a 40 second, or approximately 1 km resolution. The total area coverage extended from 14.31–20.00 $^{\circ}\text{E}$  to 29.00–34.69 $^{\circ}\text{S}$ . Cloud masking was achieved by applying a two-step thresholding algorithm to the thermal infra-red wavebands, with constant “tuning” of the threshold for each individual scene. The SST algorithm applied to the infra-red data represents SST according to the linear equation

$$\text{SST } (^{\circ}\text{C}) = (\text{digital value} \times 0.127) - 0.254 .$$

Remotely-sensed measurements of SST were used in conjunction with the SST v. integrated  $\text{NO}_3\text{-N}$  relationship (derived from *in situ* observations). Consequently, it was necessary to assess the potential effect of the sea surface skin-temperature deviation. The temperature of the sea surface is typically between 0.1 and 0.5 $^{\circ}\text{C}$  cooler than the temperature a few centimetres below, because of the vertical heat flux (Robinson 1985). A 1 $^{\circ}\text{C}$  bin size was used to group the integrated  $\text{NO}_3\text{-N}$  values in the estimation of event-scale potential new production. Therefore, the error introduced by skin effect would be minimized by the relatively broad temperature bands used in the study.

The data were analysed to give the area covered ( $\text{km}^2$ ) in the defined southern Benguela region by 10, 11, 12, 13, 14, 15 and 16 $^{\circ}\text{C}$  water. Water of 10 $^{\circ}\text{C}$  is defined as 10.00–10.99 $^{\circ}\text{C}$ .

Waldron and Probyn (1992) used the regression equation between SST and integrated  $\text{NO}_3\text{-N}$  to predict the amount of  $\text{NO}_3\text{-N}$  associated with different bands of SST in the southern Benguela during an upwelling event. In the present study, however, having obtained a statistically significant negative correlation between SST and integrated  $\text{NO}_3\text{-N}$ , the latter were grouped into 1 $^{\circ}\text{C}$  temperature bins between the range 10–16 $^{\circ}\text{C}$ . This permitted the calculation of mean integrated  $\text{NO}_3\text{-N}$  values ( $\pm\text{SD}$  and  $\text{SE}$ ) for each temperature bin. Integrated  $\text{NO}_3\text{-N}$  v. SST were then presented as a series of discrete values (with associated error) rather than a regression line.

Using the set of 10 SST satellite images and computed areas of temperature bands, it was possible to calculate the amount of  $\text{NO}_3\text{-N}$  ( $\text{mmol}$ ) in the pro-

ductive surface zone available for new production for each of the 10 upwelling events. This was converted from mmol NO<sub>3</sub>-N to gC using the Redfield ratio. The conversion was as follows:

- (i) mmol NO<sub>3</sub>-N × molar relationship between carbon and nitrogen in the marine environment (6.6) gives mmol C;
- (ii) mmol C × atomic weight of carbon (12) gives mg C;
- (iii) mg C/1 000 gives g C.

From these conversions, it was possible to provide event-scale estimates of potential new production in the southern Benguela upwelling system.

### Annual estimates of potential new production

There are a number of linked variables in the coastal region which are relevant to a dynamic consideration of upwelling. These variables include, *inter alia*, wind, cross-shelf currents and pressure-adjusted sea level at the coast. During upwelling, the prevailing equatorward wind drives an offshore surface cross-shelf current, which results in a drop in sea level at the coast. The cumulative offshore transport during an event is therefore linked to the wind strength and duration. The offshore transport is associated with nutrient-rich bottom water upwelled into the photic zone.

The satellite images chosen for event-scale estimates of new production were selected on the basis of an abundance of cold water off the west coast of South Africa in combination with cloud-free conditions. This subjective choice, from the images available from any given year, represented prominent upwelling events. The objective was to establish a quantitative relationship between a variable that is a proxy for upwelling and a variable that gauges a response to upwelling. Variables indicative of forcing were tidal-filtered, pressure-adjusted sea level at a point on the coast, and wind strength and direction at an adjacent site. The response variable was NO<sub>3</sub>-N content, estimated from the quantity of upwelling-derived water present as a result of the event.

### Sea level and wind dataset

The 1980–1990 sea level dataset was derived from de Cuevas (1986), who compiled the daily mean sea level along the Namibian and South African coasts during the period 1980–1985, supplemented from Searson (1994) to include the latter half of the decade. The methods used in the preparation of the

dataset are detailed in Searson (1994). In summary, a dataset of daily mean sea level, adjusted for the inverse barometer effect of atmospheric pressure (Schumann and Brink 1990), was obtained from measurements taken at Saldanha Bay, a coastal site adjacent to a major upwelling centre on the west coast of South Africa (Nelson and Hutchings 1983). Sea level fluctuations in such a dataset could then be attributed to wind-driven processes.

### Wind dataset

Wind data were obtained from measurements taken at Cape Columbine. Data consisted of wind speed (m·s<sup>-1</sup>) and direction at times (08:00, 14:00 and 20:00) during the period 1985–1990.

### Relationship between sea level change and NO<sub>3</sub>-N

The 10 images of SST depicting prominent upwelling events were taken during summer between 1984/85 and 1993/94. The wind records covered the period 1985–1990 and the sea level time-series spanned 1980/81–1989/90. For the purpose of establishing a relationship between the proxy and NO<sub>3</sub>-N, the overlapping period was 1984/85–1989/90. The exact dates of the satellite images during this period were: 22 February 1985; 29 January 1986; 8 January 1987; 2 February 1988; 25 January 1989; 24 January 1990.

The SST images were used to quantify the amount of NO<sub>3</sub>-N per upwelling event using the SST v. integrated NO<sub>3</sub>-N. Wind patterns and sea level fluctuations were then examined for the periods leading up to when the images were taken.

The occurrence of equatorward winds for the period prior to the upwelling images was established by examining the southerly wind component for the relevant periods. Similarly, the sea level time-series was examined to establish links between sea level fluctuation, wind and strength of upwelling. The strength of forcing (sea level fluctuation) in relation to the extent of the response (NO<sub>3</sub>-N content per event) was examined using regression and correlation analyses of the variables. Care was taken with regard to the appropriate method of regression (Ricker 1973), i.e. Model I (*Y* on *X*) or Model II (geometric mean). Having established a significant relationship, the amount of NO<sub>3</sub>-N available from other upwelling events in any given year (predicted from the fluctuation in sea level) could be calculated and summed to provide annual estimates of potential new production. This was possible for the length of the sea level record (1980/81–1989/90).

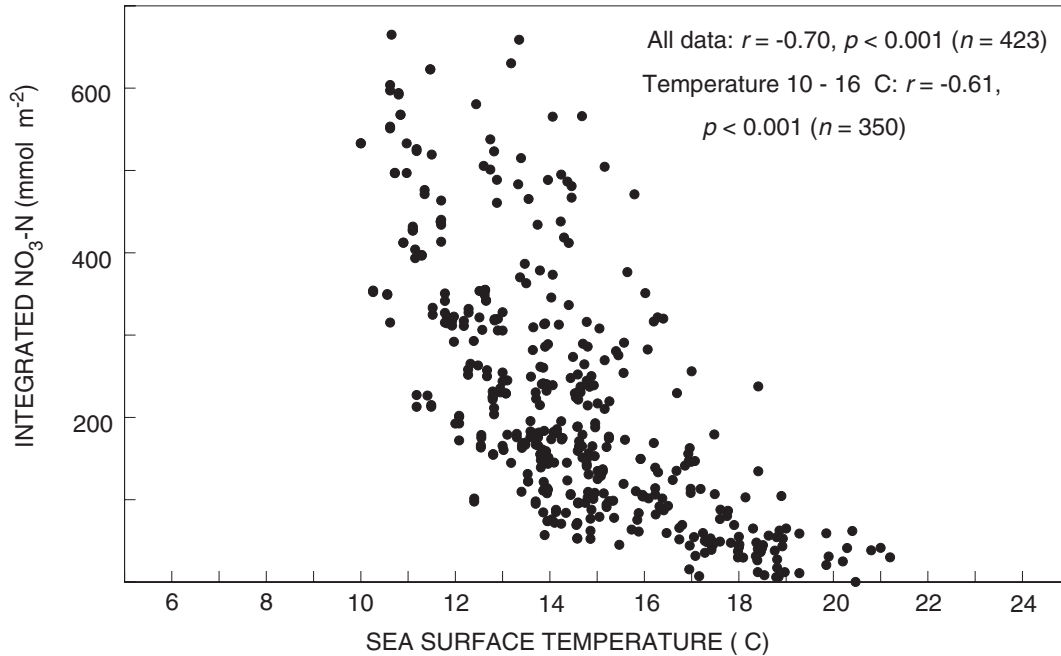


Fig. 1: Relationship between sea surface temperature and integrated  $\text{NO}_3\text{-N}$  over the upper 30 m of the water column in the southern Benguela

## RESULTS

### Relationship between SST and integrated $\text{NO}_3\text{-N}$

A significant, negative relationship between SST and integrated  $\text{NO}_3\text{-N}$  is depicted in Figure 1. The relationship is similar to that found by Zentara and Kamykowski (1977), who plotted temperature v.  $\text{NO}_3\text{-N}$  at an equivalent southern latitude ( $35^\circ\text{S}$ ) as that of the current study.

### Integrated $\text{NO}_3\text{-N}$ values associated with temperature bins between 10 and 16°C

The mean integrated  $\text{NO}_3\text{-N}$  values were computed and grouped into  $1^\circ\text{C}$  temperature bins (Table I). The confidence limits at the 95% level were estimated for each sample mean, except in the  $10^\circ\text{C}$  bin (where the number of observations was  $<30$ ), in which case the  $t$ -distribution was used for calculating the 95% confidence interval. For the bins between 13 and  $16^\circ\text{C}$ , using a standard error of difference between means, there was no significant difference

between the means of adjacent bins, although non-adjacent bins were significantly different.

### Satellite areas associated with temperature bins between 10 and 16°C

An example of four satellite images of SST depicting different upwelling events is shown in Figure 2. The computed areas ( $\text{km}^2$ ) associated with the  $1^\circ\text{C}$  bands of temperature from all 10 images are given in Table II and Figure 3.

Table I: Mean integrated  $\text{NO}_3\text{-N}$  values (0–30 m depth) for each  $1^\circ\text{C}$  sea surface temperature and their respective 0.95 levels of probability

Temperature Bin ( $^\circ\text{C}$ )	Mean integrated $\text{NO}_3\text{-N}$ ( $\text{mmol}\cdot\text{m}^{-2}$ )	$\pm$ 95% level
10	496.6	38.5
11	390.4	33.3
12	290.2	28.3
13	223.4	22.0
14	200.5	19.9
15	176.9	29.1
16	142.8	30.4

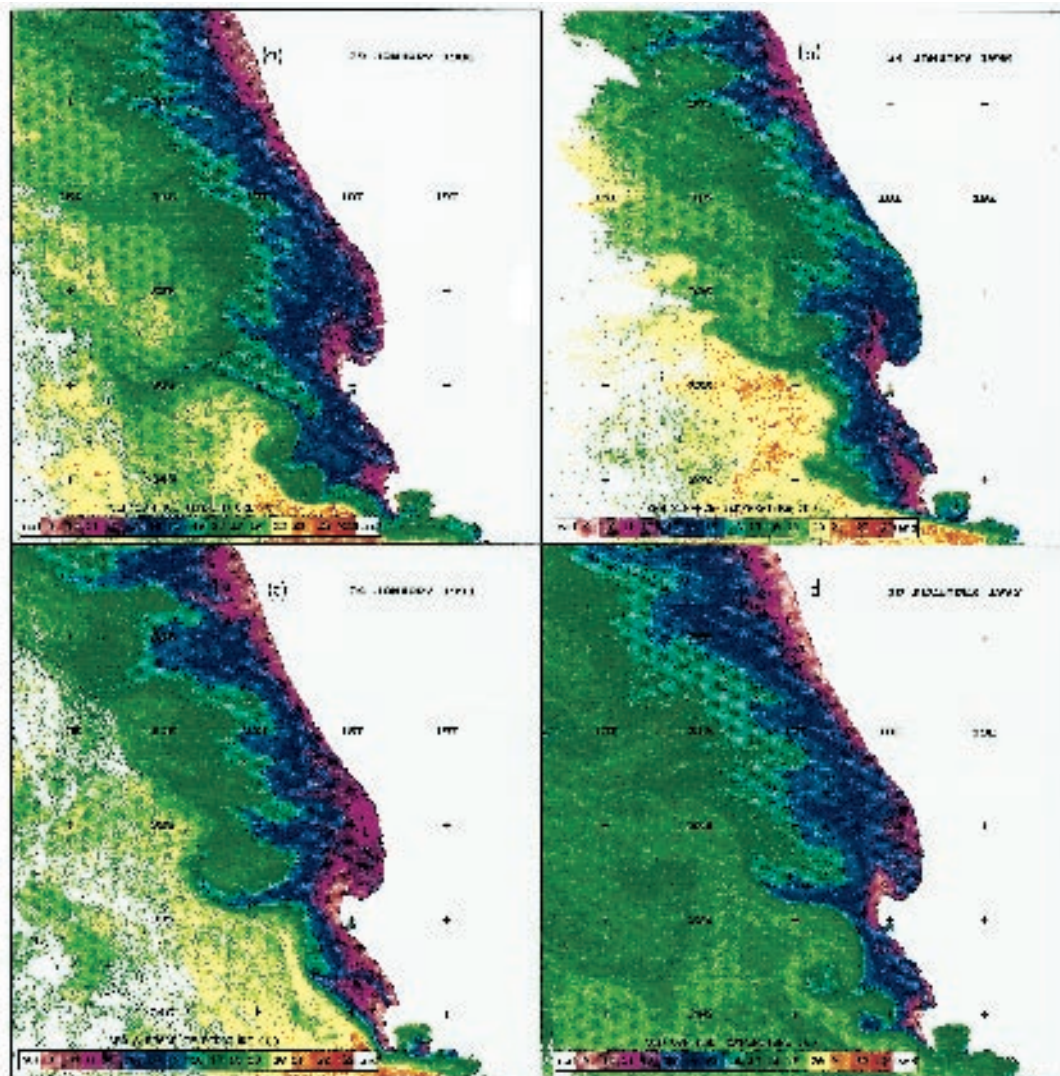


Fig. 2 TIROS/NOAA satellite images showing the surface temperature in the southern Benguela

#### Total $\text{NO}_3\text{-N}$ and potential new production per event

From the information provided in Tables I and II it was possible to calculate the amount of  $\text{NO}_3\text{-N}$  available for new production (mmols) for each of the 10 upwelling images (Table III). The mmol quantities of event-scale  $\text{NO}_3\text{-N}$  were expressed in terms of carbon, using the conversion factors given earlier in the text.

#### Wind regime and upwelling events

The southerly components of wind in the 10-day periods preceding the satellite images of SST (Fig. 4) showed the presence of upwelling-favourable, equatorward winds. The wind data represent daily measurements at 08:00. That time was selected in order to minimize the influence of land/sea breeze effects (Shannon 1985). The presence of dominant southerly winds in the period leading up to the satellite images

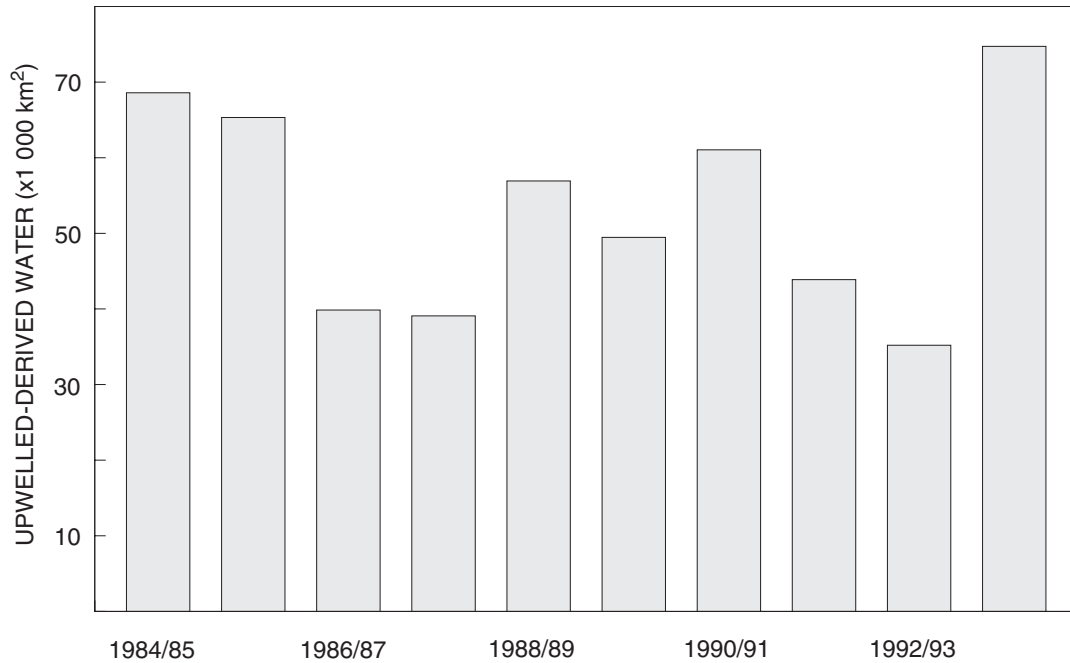


Fig. 3: Area of upwelling-derived water (10–16°C) obtained from satellite imagery for the 10 upwelling events, 1984/85–1993/94

supports the contention that the selected images followed periods of active upwelling. A quantitative link between wind and upwelling was complicated by the variability in wind over time.

#### Sea level fluctuation, upwelling events and potential new production

The record of tidal-filtered, pressure-adjusted sea

level at an adjacent coastal site in the same 10-day periods preceding the images (Fig. 5) provided alternative evidence of upwelling and showed that there were sometimes relatively large fluctuations coincident with upwelling events. It was assumed that the largest deviation from the mean in sea level, immediately prior to the upwelling image, was related to the primary forcing mechanism responsible for that event.

With the exception of 1986/87, each image was preceded by a fall then a rise in sea level. The sequence

Table II: Areas (km<sup>2</sup>) of water associated with each specific temperature band from 10 satellite images of upwelling events between 1984/85 and 1993/94

Date	Area (km <sup>2</sup> ) of water per temperature						
	10°C	11°C	12°C	13°C	14°C	15°C	16°C
22 Feb. 1985	1 111	2 955	5 822	5 057	11 979	21 949	19 712
29 Jan. 1986	2 772	4 102	5 398	9 832	11 040	13 586	18 585
08 Jan. 1987	52	294	592	1 248	3 835	12 461	21 373
02 Feb. 1989	753	1 795	2 296	5 119	8 880	9 458	10 781
25 Mar. 1989	172	979	2 107	6 707	15 068	17 158	14 738
24 Jan. 1990	720	2 518	3 672	5 156	8 639	13 110	15 653
24 Jan. 1991	3 388	5 423	8 316	7 956	9 180	11 245	15 539
05 Mar. 1992	8	137	869	4 106	7 610	15 679	15 469
14 Jan. 1993	996	1 774	3 105	6 146	6 561	7 555	9 061
10 Dec. 1993	2 085	2 804	5 238	12 016	12 713	15 476	24 392

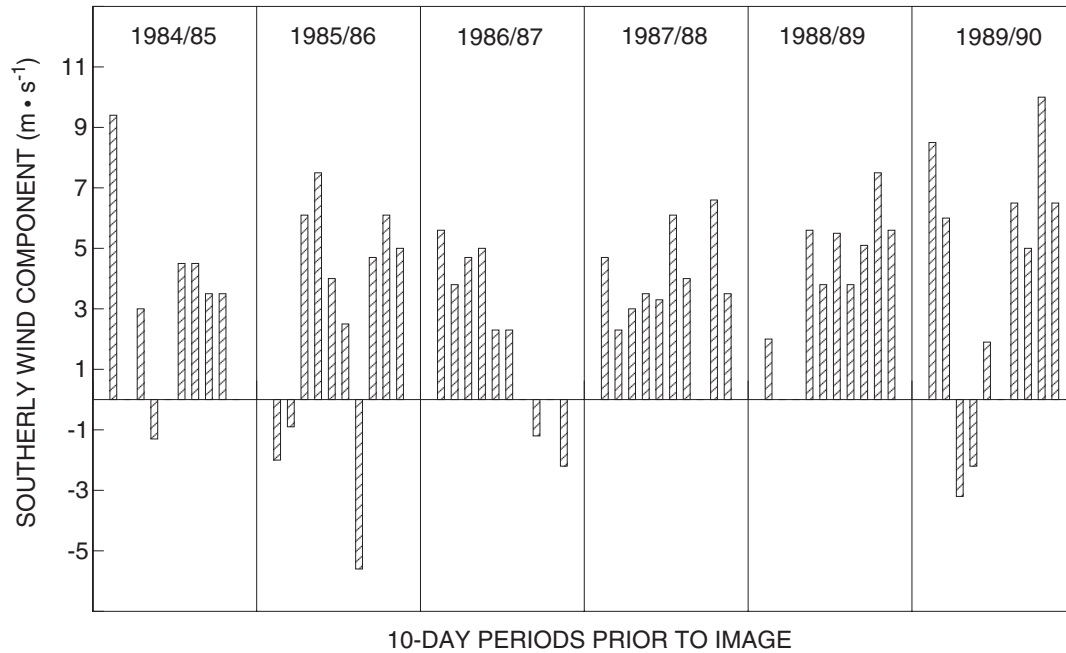


Fig. 4: Southerly wind components (measured at Cape Columbine) for a 10-day period preceding the satellite images of upwelling events, 1984/85–1989/90

of events driving the 1986/87 event appears to be more complex. The question is whether there is a quantitative link between sea level fluctuation and  $\text{NO}_3\text{-N}$  content. In this context, it was important to examine more closely the relationship between wind and sea level at the same point on the coast. In the case of wind-induced upwelling, the extent of upwelling should depend upon the intensity and duration of wind over a period of time. The stronger and longer the wind event, the greater the cumulative effect on

upwelling. This Cumulative Ekman Transport (CET) is proportional to the product of the intensity of equatorward wind and the duration of the event. CET is therefore directly linked, via the wind, to a change in sea level at the coast. The speed at which sea level changes is dependent on wind strength, whereas wind duration results in a cumulative effect on sea level.

From the record of sea level prior to each of the upwelling images and coincident with the upwelling event, the sea level fall and rise during large fluctuations was regressed against the  $\text{NO}_3\text{-N}$  content. The relationship between the fall in sea level and  $\text{NO}_3\text{-N}$  content (Fig. 6a) was not significant, whereas the relationship between rise in sea level and  $\text{NO}_3\text{-N}$  content (Fig. 6b) was significant ( $p < 0.01$ ), if the 1986/87 data point was excluded from the regression. The 1986/87 event was unusual, because the image was preceded by a prominent rise then a fall in sea level as opposed to the more characteristic fall then rise (Fig. 5). A further complication was that the sea level rose in two distinct steps, separated by a day before it fell. The alternative data points for 1986/87 plotted in Figure 6b represent (A), the total rise in sea level, ignoring the step, and (B), the second rising portion only. Given the atypical nature of this upwelling event and the alternative interpretations of its

Table III: Event-scale estimates ( $\pm$  95% confidence level) of available  $\text{NO}_3\text{-N}$  and their carbon equivalents for the 10 satellite images of upwelling events between 1984/85 and 1993/94

Year	$\text{NO}_3\text{-N}$ ( $\text{mmols} \times 10^{12}$ )	New Production ( $\text{gC} \times 10^{12}$ )
1984/85	$13.624 \pm 1.899$	$1.08 \pm 0.15$
1985/86	$14.012 \pm 1.807$	$1.11 \pm 0.14$
1986/87	$6.616 \pm 1.145$	$0.52 \pm 0.09$
1987/88	$7.878 \pm 1.050$	$0.62 \pm 0.08$
1988/89	$10.739 \pm 1.494$	$0.85 \pm 0.12$
1989/90	$9.845 \pm 1.361$	$0.78 \pm 0.11$
1990/91	$14.039 \pm 1.722$	$1.11 \pm 0.14$
1991/92	$7.735 \pm 1.198$	$0.61 \pm 0.09$
1992/93	$7.407 \pm 0.952$	$0.59 \pm 0.08$
1993/94	$15.105 \pm 2.041$	$1.20 \pm 0.16$

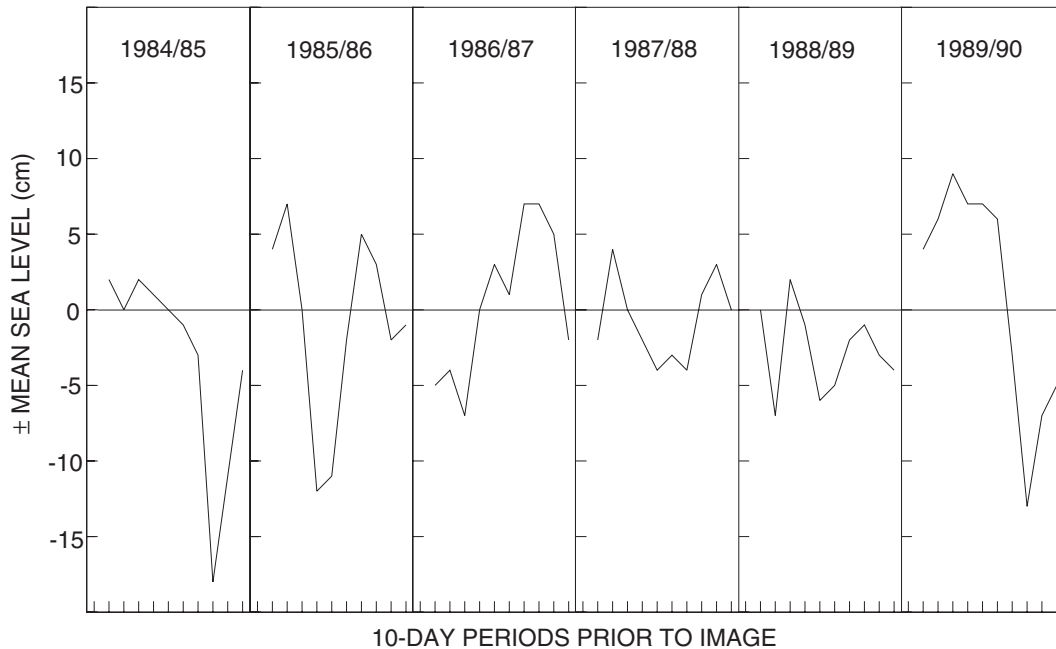


Fig. 5: Sea level fluctuation at the coast (measured at Saldanha Bay) for 10-day period preceding the satellite images of upwelling events, 1984/85–1989/90

sea level signature, they were excluded from the analysis.

The Model I regression of a simple linear equation was thought appropriate in the regression, because the  $x$ -residuals were assumed to be very small (E. T. Pelzer, Woods Hole Oceanographic Institute, pers. comm.). The  $x$  variable was the sea level rise associated with an upwelling event, which was obtained from a tide gauge (i.e. instrument-measured). Alternatively, if both  $x$  and  $y$  variables had been independent, then a functional or Model II geometric mean regression (Ricker 1973) would have been used. The regression equation (Fig. 6b) has standard errors of the  $y$ -estimate and the  $x$ -coefficient of 1.58 and 0.17 respectively.

The results indicated a positive, but possibly tenuous (because of the small sample size), relationship between the rise in sea level during an upwelling event and the quantity of  $\text{NO}_3\text{-N}$ . The quantity of  $\text{NO}_3\text{-N}$  upwelled for other events in any given year was then predicted from the event-scale rises in sea level, providing annual estimates of potential new production.

The assumption was made that there is a threshold value in the rise in sea level below which the  $\text{NO}_3\text{-N}$  introduced to the surface layer is likely to be negligible. The relationship shown in Figure 6 was based on

variables obtained from selected large upwelling events. It is not known what regressed values of event-scale  $\text{NO}_3\text{-N}$  are obtained from low values of sea level rise. Therefore, a cautious approach was adopted by regressing values of  $\text{NO}_3\text{-N}$  for sea level rises  $> 3$  cm. From the records of sea level between 1980 and 1990 and the relationship shown in Figure 6b, the annual values of potential new production ( $\text{mmol NO}_3\text{-N}\cdot\text{year}^{-1}$ ) and their carbon equivalents were calculated (Table IV).

Table IV: Annual estimates of potential new production for the 1980s, expressed in terms of  $\text{NO}_3\text{-N}$  and carbon ( $\pm 95\%$  confidence level)

Year	( $\text{mmol NO}_3\text{-N}\cdot\text{year}^{-1}$ ) $\times 10^{14}$	$\text{gC}\cdot\text{year}^{-1} \times 10^{13}$
1980/81	7.47	$5.92 \pm 1.76$
1981/82	7.27	$5.76 \pm 1.70$
1982/83	7.61	$6.03 \pm 1.78$
1983/84	7.82	$6.19 \pm 1.83$
1984/85	6.51	$5.16 \pm 1.51$
1985/86	7.03	$5.57 \pm 1.61$
1986/87	6.85	$5.43 \pm 1.58$
1987/88	6.59	$5.22 \pm 1.52$
1988/89	6.91	$5.47 \pm 1.61$
1989/90	6.51	$5.16 \pm 1.48$



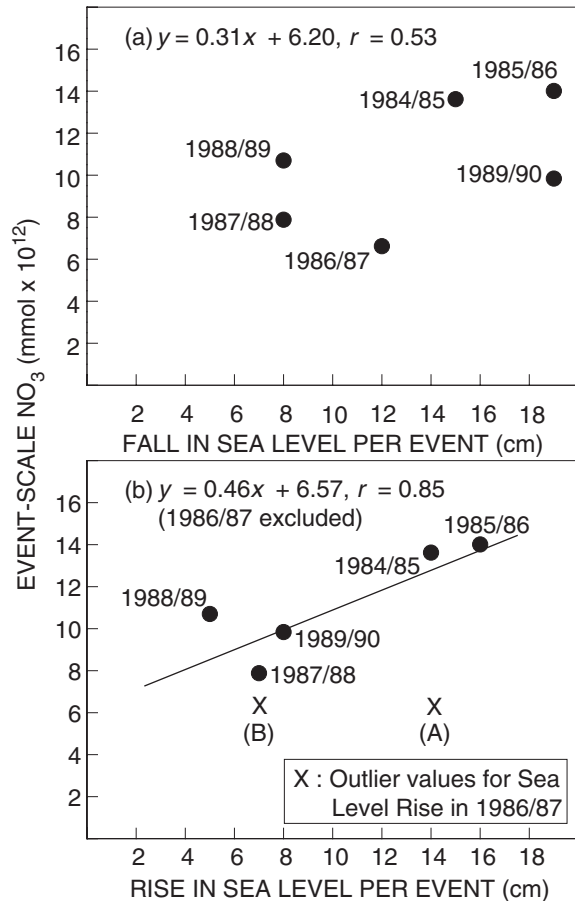


Fig. 6: Relationships between (a) fall in sea level and (b) rise in sea level at Saldanha Bay preceding the upwelling events and the amount of NO<sub>3</sub>-N associated with each event, 1984/85–1989/90

## DISCUSSION

### Event-scale estimates of potential new production

The interpretation of satellite imagery is often hampered by the fact that satellite equipment only senses the ocean surface. In the present study, a depth-related parameter (integrated NO<sub>3</sub>-N) was obtained from a surface variable (SST), which permitted the NO<sub>3</sub>-N content of the upper 30 m of the water column to be quantified at the regional level on a snapshot basis. This method of estimating the event-scale potential new production in the southern Benguela

was more direct than using algorithmically derived total production (from remotely-sensed chlorophyll *a*) in combination with a regionally appropriate *f*-ratio (e.g. Sathyendranath *et al.* 1991). Areas of uncertainty from assumptions in the method, and underlying logic, require examination. The absence of measured euphotic zone depths in the dataset necessitated the designation of 30 m as the lower boundary of the productive surface layer. The choice of the 0–30 m depth range took into account the wide range of possible euphotic zone depths generally found in coastal areas, and especially those in upwelling systems (Shannon 1985, Brown and Hutchings 1987, Estrada and Marrasé 1987). In cases where the base of the euphotic zone was below 30 m, the NO<sub>3</sub>-N content would have been underestimated. Conversely, any NO<sub>3</sub>-N that got to within 30 m of the surface would be utilized in the context of potential new production per event, because vertical transport mechanisms, such as wind mixing and Langmuir circulation, would be superimposed on the upwelling pulse. Waldron and Probyn (1992) tested the sensitivity of the potential new production to choice of depth range and found that, using the 0–40 and 0–20 m depth ranges for purposes of integration, respectively raised and lowered the final estimate by 38%, but did not alter the order of magnitude.

The temperature range of 10–17°C selected for upwelling-derived water was based on the combined works of Andrews and Hutchings (1980) and Waldron (1985). The former study showed that water lying outside the upwelling front (termed oceanic water) generally had temperatures >18°C. Waldron (1985) used salinity to tag upwelling-derived water (from approximately 200 m depth offshore) inshore of the upwelling front and found that sun-warming increased the temperature from 10 to 14°C (maturing upwelled water). Water temperatures of up to 16°C formed the inshore portion of the frontal zone, having salinities characteristic of water from approximately 100 m deep offshore.

The method used here to assess NO<sub>3</sub>-N content of the surface layer was slightly different from that used by Waldron and Probyn (1992). The mean integrated NO<sub>3</sub>-N values were used for the range of temperature bins between 10 and 16°C rather than the regressed values from the SST v. integrated NO<sub>3</sub>-N relationship. The question arises whether the integrated NO<sub>3</sub>-N values are realistic for upwelled water in the southern Benguela. SST water of 10°C had a mean integrated (0–30 m) NO<sub>3</sub>-N value of 496.6 mmol·m<sup>-2</sup>, which equates to a mean concentration of 16.6 mmol·m<sup>-3</sup> for that depth range. Such water would be of South Atlantic Central Water (SACW) origin which was recently upwelled. This compares favourably

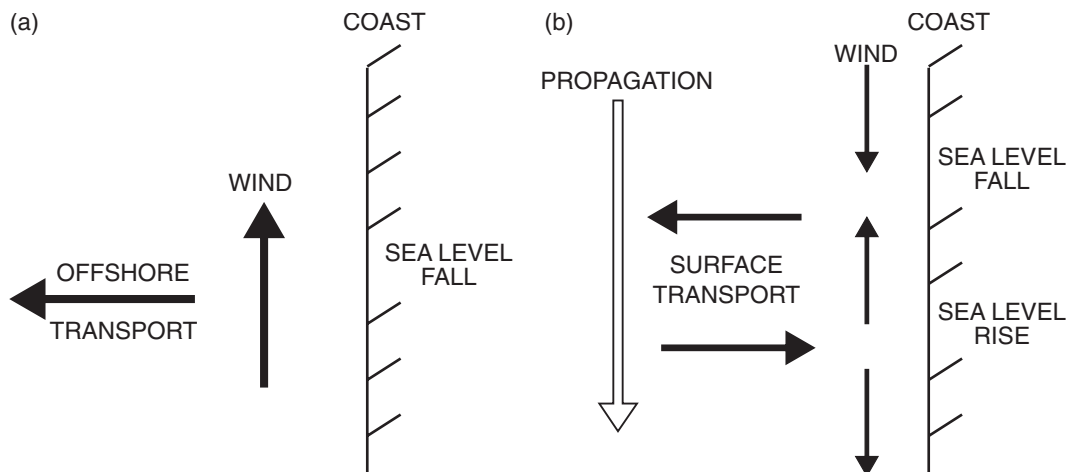


Fig. 7: Schematic representation of (a) a simple model of forcing wind systems and sea level response, which assumes uniformity around the coast, and (b) a more realistic model of upwelling dynamics

with values of  $10\text{--}15\text{ mmol}\cdot\text{m}^{-3}$  (Jones 1971) and  $10\text{--}18\text{ mmol}\cdot\text{m}^{-3}$  (Henry 1975) for SACW. Andrews and Hutchings (1980) reported southern Benguela upwelled water with  $\text{NO}_3\text{-N}$  values of  $20 \pm 4\text{ mmol}\cdot\text{m}^{-3}$ .

Potential new production estimated for the southern Benguela at the event scale ranged between  $0.52$  and  $1.20 \times 10^{12}\text{ gC}$ . Waldron and Probyn (1992) estimated the potential new production to be  $2.46 \times 10^{12}\text{ gC}$  for the combined northern and southern Benguela systems using a whole system NOAA 9 image, dated 22 March 1987.

#### First-order estimates of annual potential new production

The annual potential new production estimates for the southern Benguela using the current methodology ranged between  $5.16$  and  $6.19 \times 10^{13}\text{ gC}\cdot\text{year}^{-1}$ . Waldron and Probyn (1992) estimated  $4.7 \times 10^{13}\text{ gC}\cdot\text{year}^{-1}$  for the annual potential new production for the whole Benguela system. This value compared well with other estimates of production in different regions of the Benguela, but it did not take into account the variability in duration and intensity of upwelling events. Regional estimates of annual potential new production appear robust at the  $10^{13}$  order of magnitude.

The decadal interannual comparison given here shows that estimates can vary by 20% of the minimum. General trends in the 1980s (Table IV) show that annual potential new production in the first half of the decade was greater than in the second half, with a

substantial decrease during 1984/85. This was consistent with certain related variables reported by Shannon *et al.* (1992), in which the annual time-series of SST anomalies showed unusually cold water (and hence more available  $\text{NO}_3\text{-N}$ ) in the southern Benguela coastal zone during most of the first half of the 1980s and unusually warm water in the second half. Also, Shannon *et al.* (1992) showed a consistent trend in the sequences of annual averaged anomalies of equatorward pseudo wind stress and deviation from the monthly mean of the equatorward wind component at Cape Columbine lighthouse. From this relative comparison, it appears that sea level fluctuations are useful as a proxy for estimating annual potential new production.

A simple model of upwelling on the west coast of South Africa dictates that upwelling-favourable winds are accompanied by sea level fall at the coast as a result of Ekman transport. Such a simple model assumes a uniformity around the coast of forcing wind systems and the sea level response (Fig. 7a). In the present study, there was a significant relationship between sea level rise and quantity of  $\text{NO}_3\text{-N}$  (upwelling response). This was contrary to the above-mentioned simple model. In reality, neither wind-induced forcing nor upwelling response are uniform along the South African coast. Moreover, the forcing systems and response manifestations move in an anticlockwise direction around the coast (Schumann and Brink 1990). During periods of upwelling-favourable winds at one location, there may be weak winds or downwelling-favourable winds at neigh-

bouring locations. This may result in a sympathetic alternation between fall and rise in sea level at the coast, which is illustrated in Figure 7b. The likelihood of asynchrony can be better appreciated by considering that, in a given time-frame, the weather system and its associated pattern of offshore (sea level fall) and onshore (sea level rise) surface transport moves down and around the coast: weather systems, as a coastal trapped wave in the lower atmosphere (Gill 1977) and surface transport patterns, as a coastal trapped wave in the shelf ocean (Gill and Schumann 1974). The main generating mechanisms of coastal trapped waves are longshore winds and coastal lows, which generally move much faster than coastal trapped waves in the shelf region of the South African south coast (Schumann and Brink 1990). In their study of the complex set of interactions between forcing variables, Schumann and Brink (1990) found that, in a strongly wind-forced region, the variation in local sea level was generally more highly correlated with wind at locations in the direction from which coastal trapped waves would propagate. Therefore, the peak intensity of the different aspects of forcing and response can arrive at a point on the coast with a lag between them (Schumann and Brink 1990). The relative speed between forcing and response systems can be different and so the lags can vary. However, Nelson (1992) states that a suitable phase relationship between remotely generated coastal-trapped waves and local wind is a requirement for efficient upwelling.

The relative differences in estimates of annual potential new production during the 1980s were in broad agreement with related variables reported for the same period. The mean estimate (in absolute terms) can be compared with measurements of  $\text{NO}_3\text{-N}$  uptake (new production) in the southern Benguela taken during research cruises. The regional estimates covered an area of some tens of thousands of square kilometres, whereas uptake measurements ( $\text{m}^{-2}$ ) provide an hourly or daily rate of assimilation. This difference in scale, and hence resolution, coupled with non-synopticity, necessitated the extrapolation of measured ambient rates as a means of testing whether they can account for the regional estimates.

The four research cruises in the southern Benguela used to obtain a combined dataset of  $\text{NO}_3\text{-N}$  uptake were: March 1987 (Waldron and Probyn 1992); March 1990 (Shillington *et al.* 1992); February 1991 (Probyn *et al.* 1996); and February 1995 (Sea Fisheries Research Institute and University of Cape Town, unpublished data). The daily rates of integrated  $\text{NO}_3\text{-N}$  uptake were grouped into new, mature and aged water categories on the basis of SST (10–12, 13–14 and 15–16°C respectively). This resulted in mean daily rates of  $20.83 \text{ mmol}\cdot\text{m}^{-2}\cdot\text{day}^{-1}$  (new

water),  $15.55 \text{ mmol}\cdot\text{m}^{-2}\cdot\text{day}^{-1}$  (mature water) and  $7.70 \text{ mmol}\cdot\text{m}^{-2}\cdot\text{day}^{-1}$  (aged water). Grouping the areas ( $\text{km}^2$ ) of upwelling-derived water from the 10 satellite images of SST into the same categories, gave the following mean values:  $7\,225 \text{ km}^2$  (new water),  $15\,885 \text{ km}^2$  (mature water) and  $30\,298 \text{ km}^2$  (aged water).

Assuming that this was a consistent configuration for the upwelling region over a productive year of 274 days (which excludes winter), and converting  $\text{mmol N}$  to  $\text{gC}$ , the mean annual new production rate is estimated at  $1.4 \times 10^{13} \text{ gC}\cdot\text{year}^{-1}$ . This value compares favourably with the mean annual potential new production of  $5.6 \times 10^{13} \text{ gC}\cdot\text{year}^{-1}$  estimated in this study, confirming  $10^{13}$  as the appropriate order of magnitude. Note that potential new production assumes the total uptake of  $\text{NO}_3\text{-N}$ .

Further consideration was given to the annual potential new production estimates in the context of an intra- and inter-regional comparison. Brown *et al.* (1991) estimated the total (new and regenerated) production for the southern Benguela to be  $7.64 \times 10^{13} \text{ gC}\cdot\text{year}^{-1}$ . The mean annual potential new production estimated here is  $5.6 \times 10^{13} \text{ gC}\cdot\text{year}^{-1}$ , giving an  $f$ -ratio (new production : total production) of 0.73. From  $^{14}\text{C}$  uptake studies, Shannon and Field (1985) reported a total production rate of  $4.0 \text{ gC}\cdot\text{m}^{-2}\cdot\text{day}^{-1}$  for the Cape Columbine/St Helena Bay region. Expressing the mean estimate of annual potential new production in the same units, by applying the mean area of upwelling-derived water ( $5.34 \times 10^{10} \text{ m}^2$ ), gives a rate of  $2.87 \text{ gC}\cdot\text{m}^{-2}\cdot\text{day}^{-1}$ , which translates to an  $f$ -ratio of 0.72. These  $f$ -ratios are at the maximum of the accepted range for the southern Benguela upwelling system (Probyn 1992), because potential new production is being estimated. This daily new production rate of  $2.87 \text{ gC}\cdot\text{m}^{-2}\cdot\text{day}^{-1}$  is similar to the median rate of integrated  $\text{NO}_3\text{-N}$  uptake measured during the abovementioned four research cruises ( $29.92 \text{ mmol NO}_3\text{-N}\cdot\text{m}^{-2}\cdot\text{day}^{-1} = 2.373 \text{ gC}\cdot\text{m}^{-2}\cdot\text{day}^{-1}$ ) and to the primary production rates of 2.14 and  $3.92 \text{ gC}\cdot\text{m}^{-2}\cdot\text{day}^{-1}$  estimated by Pitcher *et al.* (1996) from determinations of  $\text{NO}_3\text{-N}$  depletion and a phytoplankton biomass-nutrient ( $\text{NO}_3\text{-N}$ ) consumption equation respectively.

The present findings show that fluctuations in sea level could be useful as a proxy for upwelling in the southern Benguela and tentatively can be related to nitrate supply. Estimates of potential new production presented here are preliminary at this stage. However, comparisons of estimates using this technique with *in situ* measured new production are reasonably good and indicate that regional nitrate supply and new production may be estimated from sea level fluctuations.

## ACKNOWLEDGEMENTS

The South African Data Centre for Oceanography, the Sea Fisheries Research Institute (SFRI) and the Satellite Applications Centre and Weather Bureau are gratefully acknowledged for supplying archived data. The SFRI is also thanked for permitting our participation in a number of their research cruises. Ms S. Weeks (University of Cape Town [UCT]) processed the satellite imagery and Ms S. Searson (UCT) and Mr R. van Ballegoyen (Council for Scientific and Industrial Research) helped in the provision of the filtered and pressure-adjusted sea level record. The work was funded by the Benguela Ecology Programme and the Department of Oceanography, University of Cape Town. The authors are grateful to Prof. R. Letelier of Oregon State University, U. S. A., and an anonymous reviewer for their comments on an earlier version of this manuscript.

## LITERATURE CITED

- ANDREWS, W. R. H. and L. HUTCHINGS 1980 — Upwelling in the southern Benguela Current. *Prog. Oceanogr.* **9**(1): 81 pp. + 2 Figures.
- BROWN, P. C. and L. HUTCHINGS 1987 — The development and decline of phytoplankton blooms in the southern Benguela upwelling system. 2. Nutrient relationships. In *The Benguela and Comparable Ecosystems*. Payne, A. I. L., Gulland, J. A. and K. H. Brink (Eds). *S. Afr. J. mar. Sci.* **5**: 393–409.
- BROWN, P. C., PAINTING, S. J. and K. L. COCHRANE 1991 — Estimates of phytoplankton and bacterial biomass and production in the northern and southern Benguela ecosystems. *S. Afr. J. mar. Sci.* **11**: 537–564.
- CHAPMAN, P. and L. V. SHANNON 1985 — The Benguela ecosystem. 2. Chemistry and related processes. In *Oceanography and Marine Biology. An Annual Review* **23**. Barnes, M. (Ed.). Aberdeen; University Press: 183–251.
- CRAWFORD, R. J. M., SHANNON, L. V. and D. E. POLLOCK 1987 — The Benguela ecosystem. 4. The major fish and invertebrate resources. In *Oceanography and Marine Biology. An Annual Review* **25**. Barnes, M. (Ed.). Aberdeen; University Press: 353–505.
- CRUICKSHANK, R. A., HAMPTON, I. and M. J. ARMSTRONG 1990 — The origin and movements of juvenile anchovy in the Orange River region as deduced from acoustic surveys. *S. Afr. J. mar. Sci.* **9**: 101–114.
- DE CUEVAS, B. A. 1986 — Daily mean sea level along the coast of Namibia and South Africa 1980–1985. *Rep. Benguela Ecol. Progm. S. Afr.* **11**: 8 pp.
- DUGDALE, R. C. and J. J. GOERING 1967 — Uptake of new and regenerated forms of nitrogen in primary productivity. *Limnol. Oceanogr.* **12**(2): 196–206.
- ESTRADA, M. and C. MARRASÉ 1987 — Phytoplankton biomass and productivity off the Namibian coast. In *The Benguela and Comparable Ecosystems*. Payne, A. I. L., Gulland, J. A. and K. H. Brink (Eds). *S. Afr. J. mar. Sci.* **5**: 347–356.
- GILL, A. E. 1977 — Coastally trapped waves in the atmosphere. *Q. Jl R. met. Soc.* **103**: 431–440.
- GILL, A. E. and E. H. SCHUMANN 1974 — The generation of long shelf waves by the wind. *J. phys. Oceanogr.* **4**(1): 83–90.
- HENRY, A. E. 1975 — Hydrology and nutrient salts of the South-East Atlantic and South-West Indian oceans in 1968. *Investl Rep. Div. Sea Fish. S. Afr.* **95**: 66 pp.
- JONES, P. G. W. 1971 — The southern Benguela Current region in February, 1966: 1. Chemical observations with particular reference to upwelling. *Deep-Sea Res.* **18**(2): 193–208.
- LUTJEHARMS, J. R. E. and J. M. MEEUWIS 1987 — The extent and variability of South-East Atlantic upwelling. In *The Benguela and Comparable Ecosystems*. Payne, A. I. L., Gulland, J. A. and K. H. Brink (Eds). *S. Afr. J. mar. Sci.* **5**: 51–62.
- McCLAIN, C. R., FU, G., DARZI, M. and J. FIRESTONE 1992 — PC-SEAPAK Users, Version 4.0, *NASA tech. Memo.* **104557**: no pagination.
- NELSON, G. 1992 — Equatorward wind and atmospheric pressure spectra as metrics for primary productivity in the Benguela system. In *Benguela Trophic Functioning*. Payne, A. I. L., Brink, K. H., Mann, K. H. and R. Hilborn (Eds). *S. Afr. J. mar. Sci.* **12**: 19–28.
- NELSON, G. and L. HUTCHINGS 1983 — The Benguela upwelling area. *Prog. Oceanogr.* **12**(3): 333–356.
- PITCHER, G. C., RICHARDSON, A. J. and J. KORRÜBEL 1996 — The use of sea temperature in characterizing the mesoscale heterogeneity of phytoplankton in an embayment of the southern Benguela upwelling system. *J. Plankt. Res.* **18**: 643–657.
- PROBYN, T. A. 1992 — The inorganic nitrogen nutrition of phytoplankton in the southern Benguela: new production, phytoplankton size and implications for pelagic foodwebs. In *Benguela Trophic Functioning*. Payne, A. I. L., Brink, K. H., Mann, K. H. and R. Hilborn (Eds). *S. Afr. J. mar. Sci.* **12**: 411–420.
- PROBYN, T. A., WALDRON, H. N., SEARSON, S. and N. J. P. OWENS 1996 — Diel variability in nitrogenous nutrient uptake at photic and sub-photoc depths. *J. Plankt. Res.* **8**(11): 2063–2079.
- RICKER, W. E. 1973 — Linear regressions in fishery research. *J. Fish. Res. Bd Can.* **30**(3): 409–434.
- ROBINSON, I. S. 1985 — Sea-surface temperature from infrared scanning radiometers. In *Satellite Oceanography: an introduction for Oceanographers and Remote-sensing Scientists*. Allan, T. D. (Ed.): 210–214.
- SATHYENDRANATH, S., PLATT, T., HORNE, E. P. W., HARRISON, W. G., ULLOA, O., OUTERBRIDGE, R. and N. HOEPPFNER 1991 — Estimation of new production in the ocean by compound remote sensing. *Nature, Lond.* **353**(6340): 129–133.
- SCHUMANN, E. H. and K. H. BRINK 1990 — Coastal-trapped waves off the coast of South Africa: generation, propagation and current structures. *J. phys. Oceanogr.* **20**: 1206–1218.
- SEARSON, S. 1994 — Extreme sea levels around the coast of southern Africa. M.Sc. thesis, University of Cape Town: 101 pp.
- SHANNON, L. V. 1966 — Hydrology of the south and west coasts of South Africa. *Investl Rep. Div. Sea Fish. S. Afr.* **58**: 22 pp. + 30 pp. of Figures.
- SHANNON, L. V. 1985 — The Benguela ecosystem. 1. Evolution of the Benguela, physical features and processes. In *Oceanography and Marine Biology. An Annual Review* **23**. Barnes, M. (Ed.). Aberdeen; University Press: 105–182.
- SHANNON, L. V., CRAWFORD, R. J. M., POLLOCK, D. E., HUTCHINGS, L., BOYD, A. J., TAUNTON-CLARK, J., BADENHORST, A., MELVILLE-SMITH, R., AUGUSTYN, C. J., COCHRANE, K. L., HAMPTON, I., NELSON, G., JAPP, D. W. and R. J. Q. TARR 1992 — The 1980s - a decade of change in the Benguela ecosystem.

- tem. In *Benguela Trophic Functioning*. Payne, A. I. L., Brink, K. H., Mann, K. H. and R. Hilborn (Eds). *S. Afr. J. mar. Sci.* **12**: 271–296.
- SHANNON, L. V. and J. G. FIELD 1985 — Are fish stocks food-limited in the southern Benguela pelagic ecosystem? *Mar. Ecol. Prog. Ser.* **22**(1): 7–19.
- SHANNON, L. V. and S. C. PILLAR 1986 — The Benguela ecosystem. 3. Plankton. In *Oceanography and Marine Biology. An Annual Review* **24**. Barnes, M. (Ed.). Aberdeen; University Press: 65–170.
- SHILLINGTON, F. A., HUTCHINGS, L., PROBYN, T. A., WALDRON, H. N. and W. T. PETERSON 1992 — Filaments and the Benguela frontal zone: offshore advection or recirculating loops? In *Benguela Trophic Functioning*. Payne, A. I. L., Brink, K. H., Mann, K. H. and R. Hilborn (Eds). *S. Afr. J. mar. Sci.* **12**: 207–218.
- WALDRON, H. N. 1985 — Influences on the hydrology of the Cape Columbine/St. Helena Bay region. M.Sc. thesis, University of Cape Town: 138 pp.
- WALDRON, H. N. and T. A. PROBYN 1992 — Nitrate supply and potential production in the Benguela upwelling system. In *Benguela Trophic Functioning*. Payne, A. I. L., Brink, K. H., Mann, K. H. and R. Hilborn (Eds). *S. Afr. J. mar. Sci.* **12**: 29–39.
- ZENTARA, S-J. and D. KAMYKOWSKI 1977 — Latitudinal relationships among temperature and selected plant nutrients along the west coast of North and South America. *J. mar. Res.* **35**: 321–337.